Terahertz electro-optic properties of $PbZr_{0.52}Ti_{0.48}O_3$ and $BaTiO_3$ ferroelectric thin films

Article *in* Applied Physics Letters · September 2014

Impact Factor: 3.3 · DOI: 10.1063/1.4896036

6 authors, including:

Dong-wen Zhang

National University of Defense Technology

30 PUBLICATIONS **76** CITATIONS

SEE PROFILE

Jianmin Yuan

National University of Defense Technology

233 PUBLICATIONS **1,858** CITATIONS

SEE PROFILE

Terahertz electro-optic properties of PbZr0.52Ti0.48O3 and BaTiO3 ferroelectric thin films

Lei Chen, Yuan Zhang, Quan Guo, Dongwen Zhang, Xiangli Zhong, and Jianmin Yuan

Citation: Applied Physics Letters **105**, 112903 (2014); doi: 10.1063/1.4896036
View online: http://dx.doi.org/10.1063/1.4896036
View Table of Contents: http://scitation.aip.org/content/aip/journal/apl/105/11?ver=pdfcov
Published by the AIP Publishing

Terahertz electro-optic properties of $PbZr_{0.52}Ti_{0.48}O_3$ and $BaTiO_3$ ferroelectric thin films

Lei Chen,[1] Yuan Zhang,[2] Quan Guo,[1] Dongwen Zhang,[1] Xiangli Zhong,[2] and Jianmin Yuan[1,a)]

[1]*Department of Physics, College of Science, National University of Defense Technology, Changsha, Hunan 410073, People's Republic of China*

[2]*School of Materials Science and Engineering, Xiangtan University, Xiangtan, Hunan 411105, People's Republic of China*

(Received 29 August 2014; accepted 6 September 2014; published online 17 September 2014)

Electro-optic effects of $PbZr_{0.52}Ti_{0.48}O_3$ (PZT) and $BaTiO_3$ (BTO) ferroelectric thin films in the terahertz frequency range are studied with high-sensitive terahertz time-domain spectroscopy. A linear response of PZT film with the linear electro-optic coefficient $r_c = 6.73 \times 10^{-11}$ m/V and a quadratic response of BTO film with the second-order electro-optic coefficient $R_c = 1.42 \times 10^{-17}$ m^2/V^2 are observed at the frequency of 1 terahertz under the applied static electric field less than 80 kV/cm. The calculation of r_c and R_c based on the Landau-Devonshire free energy theory explains the different electro-optic effects of PZT and BTO well. © *2014 AIP Publishing LLC*.
[http://dx.doi.org/10.1063/1.4896036]

Terahertz (THz) communication has been proposed as a promising way to further improve the transmission rate and capacity due to its higher carrier frequency.[1–4] Although THz communication has many advantages over optical fiber and microwave communications,[5] it has not been widely used in our daily life due to the lack of mature devices, such as effective THz external modulators.[6] The ferroelectric thin films, with large nonlinear polarizabilities and electro-optic coefficients,[7–9] are good candidates for ultrafast nonvolatile memory devices because of their extraordinary properties such as short time response to electric field, deep polarization modulation, and high detection bandwidth,[10,11] especially its stable dielectric constant in the THz band, so the ferroelectric is the ideal material for developing THz electro-optic devices.

$PbZr_{0.52}Ti_{0.48}O_3$ (PZT) is a very promising candidate for ferroelectric nonvolatile memory devices because of the low coercive field and large remanent polarizations.[12] $BaTiO_3$ (BTO) in the tetragonal ferroelectric phase at room temperature is the simplest perovskite structure in ferroelectrics.[13,14] Barium titanate based materials are critically important to the study of the electro-optic effects because of their perfect electro-optic and nonlinear optical properties.[8,9] Kim *et al*. have prepared $Ba_{0.6}Sr_{0.4}TiO_3$ thin films on MgO, which have a huge birefringence variation up to 9% at the wavelength of 632.8 nm,[9] while research on electro-optic effects of PZT and BTO films has mainly been done in visible range, but just a few in terahertz range.

In our work, we prepare PZT and BTO ferroelectric films and study their material characteristics and electro-optic effects in the THz frequency range by measuring the electric field induced birefringence with a terahertz time-domain spectroscopy (THz-TDS).[15] Compared to the traditional light intensity detection methods, TDS is more sensitive to the small change of the reflective index of samples by coherently detecting electric field of THz waves.[16] Our findings indicate that these two materials are potential candidates of THz modulators.

The epitaxial PZT and BTO thin films are fabricated by pulsed laser deposition on 0.5-mm thick $SrTiO_3$(STO) substrates.[14,17] The growth temperature, oxygen partial pressure for PZT and BTO are kept at 700 °C, 160 mTorr and 800 °C, 5 mTorr, respectively. Two different sandwich structures of films/platinum (Pt)/STO and films/$SrRuO_3$(SRO)/STO, as shown inset in Fig. 1, are used to study the electro-optic effects in the THz frequency range and characterize the material properties, respectively. The Pt coplanar electrodes spaced 100 μm are deposited by electron beam evaporation on the substrate aligned along the [010] axis with the thickness of about 40 nm. The epitaxial SRO bottom electrodes are deposited under 10 mTorr and 700 °C. The crystal structure and epitaxial relationship are examined by X-ray diffraction (XRD) and high-resolution transmission electron microscopy (HRTEM). The ferroelectric test system (RT Precision workstation) is used to study the polarization-electric (P-E) field hysteresis of the ferroelectric films.

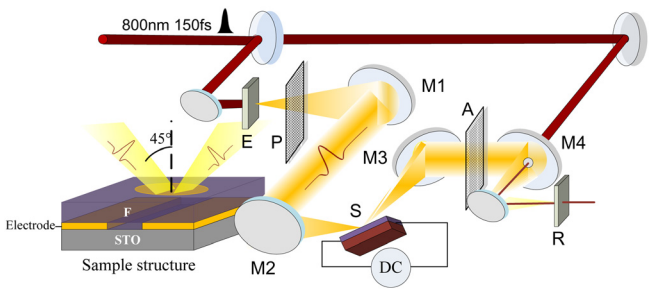

FIG. 1. The schematic diagram of THz-TDS for measuring the electro-optic effects in sample films. E: THz emitter, R: THz receiver, S: sample, M1 ~ M4: parabolic mirrors, P: THz polarizer, A: THz analyzer, DC: direct current source. The inset is the structure diagram of the sample. F: ferroelectric film.

a)Author to whom correspondence should be addressed. Electronic mail: jmyuan@nudt.edu.cn

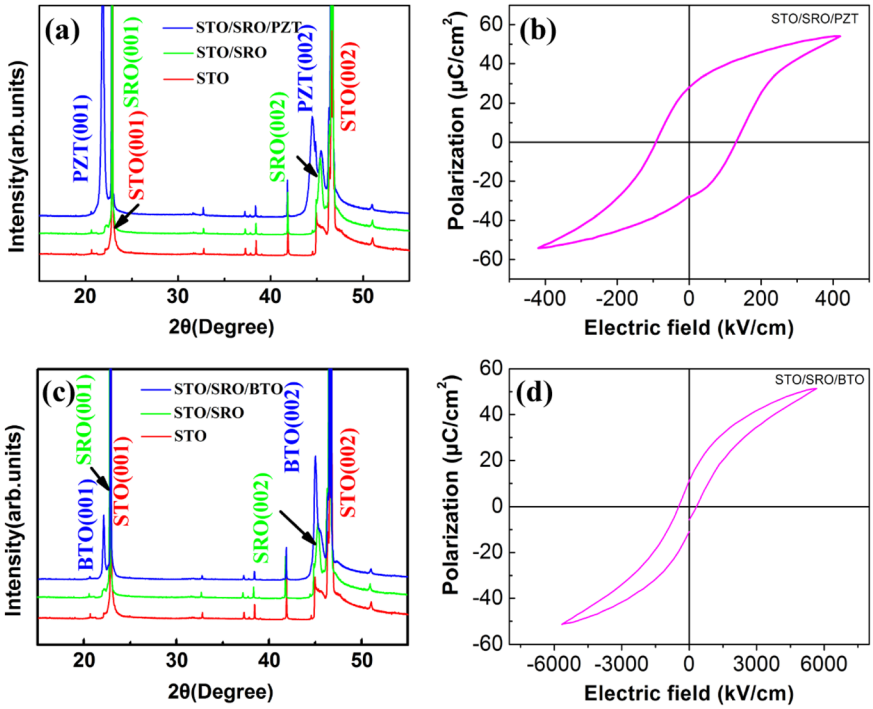

FIG. 2. The properties characterized by XRD and RT Precision workstation. The XRD patterns of PZT (a) and BTO (c) films; The P-E curves of PZT (b) and BTO (d) thin films.

A THz-TDS is used to characterize the electro-optic effects by measuring static electric field induced birefringence, as shown in Fig. 1. The optical beam (800 nm, 150 fs, 10 nJ, 76 MHz) is split into two parts, one of which goes through a translational stage to provide a relative time delay between the two arms.[18] The optical pump pulses illuminate the 1-mm thick ZnTe and generate THz pulses, which are focused on the sample and are collected by an off-axis parabolic mirror. Then, the THz pulses and the synchronized sampling probe pulses converge on the THz receiver, which ensures that the THz electric-field elliptically polarizes the probe pulses based on the electro-optic sampling principle. The probe pulses passing through the THz receiver are detected by a pair of photodiodes after passing through a $\lambda/4$ plate and a wollaston prism. Then, the signal is fed to a lock-in amplifier and computer.[19]

Reflective geometry is exploited in the specular direction, as the substrate material STO of the sample has a strong absorption of THz. The THz polarizer and analyzer located between the parabolic mirrors are used to ensure that the THz polarization direction is parallel to the horizontal plane. The THz pulses passing through the THz polarizer shine on the film between the two Pt electrodes with an angle of 45° become elliptically polarized after reflecting from the sample because of the birefrigent effect, and only the horizontally polarized component can be detected. To avoid the influence of the coercivity, we use virgin samples, in which no external electric field has yet been applied in the measurements.

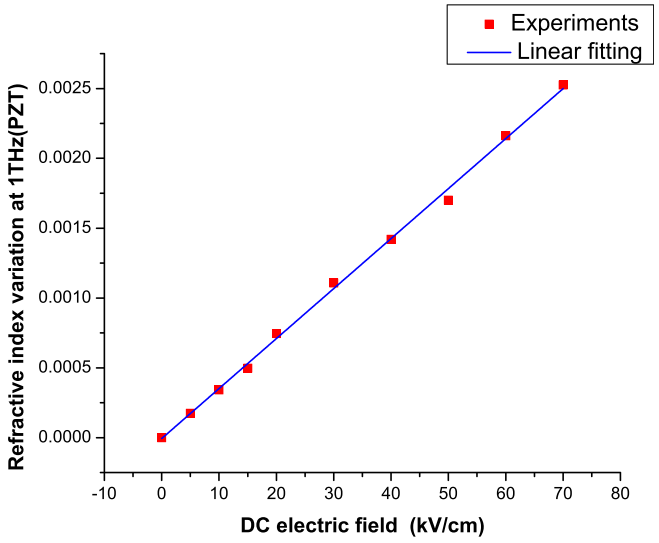

FIG. 3. Field induced birefringence of the (001)-oriented PZT thin film in an external electric field of up to 70 kV/cm. Red square dots are the experimental value. Blue line is the linear fitting curve.

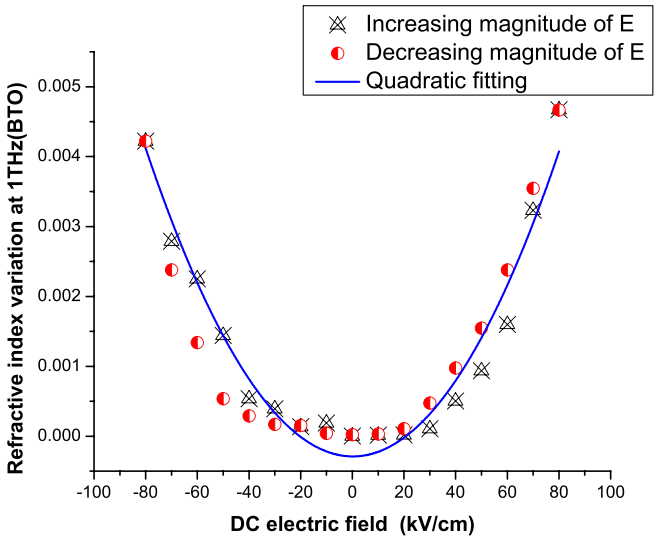

FIG. 4. Electro-optic response of the (001)-oriented BTO thin film in an external electric field of up to 80 kV/cm. Black triangle dots are experimental value of field increasing process. Red circle dots are experimental value of field decreasing process. Blue line is the polynomial fitting curve.

TABLE I. The comparison of P_r, r_c, and R_c between the experiments and the calculations.

	P_r (μC/cm^2)		r_c (m/V)		R_c (m^2/V^2)	
Sample	Experimental	Calculated	Experimental	Calculated	Experimental	Calculated
PZT/STO	28	34	6.73×10^{-11}	7.77×10^{-11}	…	7.16×10^{-19}
BTO/STO	10	12	…	8.27×10^{-12}	1.42×10^{-17}	1.59×10^{-17}

The XRD patterns of PZT and BTO films shown in Figs. 2(a) and 2(c) indicate both PZT and BTO are grown along the (001) direction without any secondary phases. The HRTEM results reveal that heterostructures of PZT/SRO and BTO/SRO are coherent without any obvious intermixing and of good epitaxial quality,[20] and the thickness of PZT and BTO films are 215 nm and 80 nm, respectively. The lattice parameters of PZT and BTO are calculated from HRTEM to be $a(\mathrm{PZT}) = b(\mathrm{PZT}) = 0.402$ nm, $c(\mathrm{PZT}) = 0.420$ nm; $a(\mathrm{BTO}) = b(\mathrm{BTO}) = 0.394$ nm, $c(\mathrm{BTO}) = 0.398$ nm, respectively. Figs. 2(b) and 2(d) show the P-E curves of PZT and BTO thin films, which indicate that both of them have good ferroelectric properties. The remanent polarizations and coercive field of PZT and BTO thin films are about $P_r(\mathrm{PZT}) = 28\ \mu\mathrm{C/cm}^2$, $E_c(\mathrm{PZT}) = 95$ kV/cm; $P_r(\mathrm{BTO}) = 10\ \mu\mathrm{C/cm}^2$, $E_c(\mathrm{BTO}) = 500$ kV/cm, respectively.

In our experiments, the static field induced refractive index variation Δn of the sample, which is proportional to the horizontal component of the THz intensity,[7,18] is measured as a function of the static electric field E at room temperature, and the results are shown in Figs. 3 and 4, respectively.

Fig. 3 shows the refractive index variation as a function of applied field for PZT thin film on STO. The data exhibits predominantly a linear electro-optic response under the electric field, with a maximum Δn of 2.52×10^{-3} when $E = 70$ kV/cm. According to the linear fitting curve of $\Delta n = 3.58 \times 10^{-5} E$, we can get the linear electro-optic coefficient of the film $r_c = 6.73 \times 10^{-11}$ m/V.

Fig. 4 depicts the birefringence variation of the BTO thin films. A predominantly quadratic and slightly asymmetric electro-optic behavior is observed for the film. The field-induced Δn starts from zero and increases continuously up to 4.22×10^{-3} when E equals 80 kV/cm. The second-order electro-optic coefficient is $R_c = 1.42 \times 10^{-17}$ m^2/V^2, which can be calculated from the quadratic fitting curve of $\Delta n = 6.85 \times 10^{-7} E^2 - 1.9 \times 10^{-4}$. It is interesting that the two measurements do not overlap with each other when the electric field is either increasing or decreasing, which indicates an obvious ferroelectric hysteresis phenomenon, while the electric hysteresis being about 10 kV/cm.

With Landau-Devonshire free energy theory, we calculate the electro-optic coefficients of PZT and BTO films using the parameters acquired from the performance measurement. The knowledge of the potential $G_{LD}(T, P, u_m)$ as a function of temperature T, polarization P_i, and mismatch strain u_m enables the complete thermodynamic description of the films.[21–23] Based on the well-known expression for the elastic Gibbs function of a "cubic" ferroelectric, we add the term of external electric field E to the thermodynamic potential $G_{LD}(T, P, u_m)$,[24] which can be written as

$$G_{LD}(T, P, u_m) = G_0 + a_1^* P^2 + a_{11}^* P^4 + a_{111} P^6 + \frac{u_m^2}{s_{11} + s_{12}} - EP, \quad (1)$$

where G_0 is the free energy of paraelectric phase, a_{ijk}^* is the modified rigidity coefficient of the sample,[25] s_{ij} is the electrostrictive coefficient, and P is the polarization induced by the external electric field E.[22,26] We calculate the critical thickness for dislocation formation and replace a_{ijk} and u_m with equivalent lattice constants and equivalent misfit strain.[27–29] With the remanent polarizations (P_r, when $E = 0$) and the electric field induced polarizations (P_E, when $E \neq 0$), we obtain the linear polarization coefficient f and the second-order polarization coefficient g, which indicate the linear electro-optic coefficient r_c of Pockels effect and the second-order electro-optic coefficient R_c of Kerr effect, respectively, as

$$\begin{aligned} r_c &= f(\varepsilon - \varepsilon_0) \approx f\varepsilon, \\ R_c &= g(\varepsilon - \varepsilon_0)^2 \approx g\varepsilon^2, \end{aligned} \quad (2)$$

where ε is sample's dielectric constant at THz frequency domain. According to the above method, parameters of P_r, r_c, and R_c are calculated, as shown in Table I.

The results show that electro-optic coefficients can be simulated according to the Landau-Devonshire free energy theory. The theoretical results of remanent polarizations are in good agreement with experimental results. The ratio of r_c and R_c of PZT is about 5×10^3 times larger than that of BTO, so that the PZT thin film exhibits a linear behavior as r_c is the leading factor of the final electro-optic effects while the BTO thin film shows a quadratic behavior as R_c plays the most important role in the final electro-optic effects under the external electric field which is less than 10^7 V/m.

In conclusion, epitaxial PZT and BTO ferroelectric thin films are deposited on STO(001) substrates using the pulsed laser deposition method. Obvious electro-optic effects are observed in the THz frequency range. The PZT film exhibits a linear electro-optic effect while a predominantly quadratic and slightly asymmetric electro-optic behavior is observed for the BTO film. We also observe an obvious ferroelectric hysteresis phenomenon in BTO film in our experiments. The calculated electro-optic coefficients of the film samples in the terahertz range by means of the Landau-Devonshire free energy theory agree well with the experimental measurements.

This work was supported by the National Natural Science Foundation of China under Grant Nos. 11104352 and 11372266.

[1]J. Federici and L. Moeller, J. Appl. Phys. **107**, 111101 (2010).
[2]A. Masahiro and S. Safumi, IEICE Electron. Express **8**, 14 (2011).
[3]S. Koenig, D. Lopez-Diaz, J. Antes, F. Boes, R. Henneberger, A. Leuther, A. Tessmann, R. Schmogrow, D. Hillerkuss, R. Palmer, T. Zwick, C. Koos, W. Freude, O. Ambacher, J. Leuthold, and I. Kallfass, Nat. Photonics **13**, 275 (2013).
[4]D. W. Zhang, Z. H. Lü, C. Meng, X. Y. Du, Z. Y. Zhou, Z. X. Zhao, and J. M. Yuan, Phys. Rev. Lett. **109**, 243002 (2012).
[5]K. Ishigaki, M. Shiraish, S. Suzuki, M. Asada, N. Nishiyama, and S. Arai, Electron. Lett. **48**(10), 582 (2012).
[6]W. L. Chan, H. T. Chen, A. J. Taylor, I. Brener, M. J. Cich, and D. M. Mittleman, Appl. Phys. Lett. **94**, 213511 (2009).
[7]D. H. Reitze, E. Haton, R. Ramesh, S. Etemad, D. E. Leaird, T. Sands, Z. Karim, and A. R. Tanguay, Jr., Appl. Phys. Lett. **63**, 596 (1993).
[8]D. Y. Wang, J. Wang, H. L. W. Chan, and C. L. Choy, J. Appl. Phys. **101**, 043515 (2007).
[9]D. Y. Kim, S. E. Moon, E. K. Kim, S. J. Lee, J. J. Choi, and H. E. Kim, Appl. Phys. Lett. **82**, 1455 (2003).
[10]Y. H. Xu, *Ferroelectric Materials and their Applications* (Elsevier Science Publishers, Amsterdam, 1991).
[11]I. F. Scott and C. A. Paz de Arajuo, Science **246**, 1400 (1989).
[12]R. Ramesh, A. Inam, W. K. Chan, B. Wilkens, K. Myers, K. Remschnig, D. L. Hart, and J. M. Tarascon, Science **252**, 944 (1991).
[13]W. Jo, H. J. Cho, T. W. Noh, B. I. Kim, D. Y. Kim, Z. G. Khim, and S. I. Kwunl, Appl. Phys. Lett. **63**, 2198 (1993).
[14]E. K. Kim, S. E. Moon, S. J. Lee, S. K. Han, K. Y. Kang, and W. J. Kim, Ferroelectrics **272**, 237 (2002).
[15]Z. H. Lü, D. W. Zhang, Z. Y. Zhou, L. Sun, Z. X. Zhao, and J. M. Yuan, Appl. Opt. **51**, 676 (2012).
[16]K. Sakai, *Terahertz Optoelectronics* (Springer Science and Business Media, Berlin, Heidelberg, 2005).
[17]R. Ramesh, A. Inam, W. K. Chan, F. Tillerot, B. Wilkens, C. C. Chang, T. Sands, J. M. Tarascon, and V. G. Keramidas, Appl. Phys. Lett. **59**, 3542 (1991).
[18]Y. S. Lee, *Principles of Terahertz Science and Technology* (Springer Science and Business Media, Dordrecht, New York, 2009).
[19]X. C. Zhang and J. Z. Xu, *Introduction to THz Wave Photonics* (Springer Science and Business Media, Dordrecht, London, 2010).
[20]A. P. Chen, F. Khatkhatay, W. Zhang, C. Jacob, L. Jiao, and H. Wang, J. Appl. Phys. **114**, 124101 (2013).
[21]N. A. Pertsev, A. G. Zembilgotov, and A. K. Tagantsev, Phys. Rev. Lett. **80**, 1988 (1998).
[22]M. J. Haun, E. Furman, S. J. Jang, H. A. McKinstry, and L. E. Cross, J. Appl. Phys. **62**, 3331 (1987).
[23]A. Amin, L. E. Cross, and R. E. Newnhanm, Ferroelectrics **37**, 647 (1981).
[24]Y. L. Wang, T. R. Wei, B. T. Liu, and Z. C. Deng, Chin. Phys. Soc. **56**, 5 (2007), available at http://wulixb.iphy.ac.cn/CN/Y2007/V56/I5/2931.
[25]A. Amin, L. E. Cross, and R. E. Newnhanm, Ferroelectrics **99**, 145 (1989).
[26]V. Nagarajan, A. Stanishevsky, L. Chen, T. Zhao, B. T. Liu, J. Melngailis, A. L. Roytburd, J. Finder, Z. Yu, R. Droopad, K. Eisenbeiser, and R. Ramesh, Appl. Phys. Lett. **81**, 4215 (2002).
[27]N. A. Pertsev, V. G. Kukhar, H. Kohlstedt, and R. Waser, Phys. Rev. B. **67**, 054107 (2003).
[28]X. D. Qi, M. Wei, Y. Lin, Q. Jia, D. Zhi, J. H. Dho, M. G. Blamire, and J. L. MacManus-Driscoll, Appl. Phys. Lett. **86**, 071913 (2005).
[29]J. S. Speck and W. J. Pompe, J. Appl. Phys.**76**, 466 (1994).